Chapter 26
Applied Theory of the Vibration of Inhomogeneously Polarized Axisymmetric Bimorph Piezoelements

Arkadiy Soloviev, Pavel Oganesyan, Pavel Romanenko, Le Van Duong and Olga Lesnjak

Abstract Piezoelectric generators (PEG) are effective for energy harvesting in machines vibrating elements. Using inhomogenously polarized piezoelements in PEG allows one to increase its output characteristics (output electric potential and output power). The paper considers piezoelements, which are circular multilayer plates (bimorphs), consisting of piezoceramic layers with inhomogeneous polarization (in thickness and in radial direction). Such a method of polarization makes it possible to use a piezomodule d_{33} for bending vibrations, which is significantly larger than piezomodule d_{31}. PEG optimization can be performed on the base of mathematical modeling of the process. Linear electroelastic theory, implemented in ACELAN and ANSYS software, was used as mathematical model. Moreover, the applied theory of axisymmetric bending vibrations with a piecewise constant polarization was created. In the applied theory, hypotheses about the distribution of displacements and electric potential along the thickness of the piezoelectric element have been adopted. System of ordinary differential equations and boundary conditions for steady bending vibrations for deflection and electric potential, depending on the radial coordinate, has been formulated. A series of calculations was performed in which resonance frequencies, antiresonance and output characteristics of PEG were determined depending on the design parameters.

A. Soloviev (✉) · O. Lesnjak
Department of Theoretical and Applied Mechanics, Don State Technical University, Rostov-on-Don, Russia
e-mail: solovievarc@gmail.com

P. Oganesyan · P. Romanenko
I. I. Vorovich Mathematics, Mechanics and Computer Sciences Institute, Southern Federal University, Rostov-on-Don, Russia

L. Van Duong
Department of Mechanical Engineering and Energy, Transportation Le Quy Don Technical University, Ha Noi, Vietnam

I. A. Parinov et al. (eds.), *Advanced Materials*, Springer Proceedings in Physics 207, https://doi.org/10.1007/978-3-319-78919-4_26

26.1 Introduction

Simulation of the performance of PEG energy harvesting devices can be carried out on the base of finite element modeling in computer software such as ACELAN, ANSYS, etc. Experimental and numerical studies of PEG of stack and bimorph types are discussed in [1–4]. The ACELAN software implemented the possibility of calculating the process of polarization of piezoelectric elements based on the theory developed in [5]. The use of inhomogeneously polarized piezoelements in the bimorph type of PEG significantly increases its output characteristics [6]. In [7–10], a method for inhomogeneous polarization of rectangular bimorph piezoelements was developed and an applied theory of calculating its cylindrical bending vibrations for piecewise constant polarization was constructed. In this paper we consider axisymmetric vibrations of a bimorph piezoelement in the form of a multilayer circular disk with piezoceramic layers are partially covered with electrodes and are inhomogeneously polarized, with circular and annular regions with a thickness polarization (they are covered with electrodes along one flat face) and an electrically-connected annular section between them with radial polarization (Fig. 26.1).

26.1.1 Research Purpose

The efficiency of PEG with the shape of a bimorph circular plate with axisymmetric bending vibrations is studied. The piezoceramic layer of the transducer has an inhomogeneous polarization.

26.1.2 Research Scope

At this study, we consider the following frameworks of the problem:

(i) Inhomogeneous polarization creation technology and PEG design;
(ii) Applied theory of flexural axisymmetric vibrations of PEG;

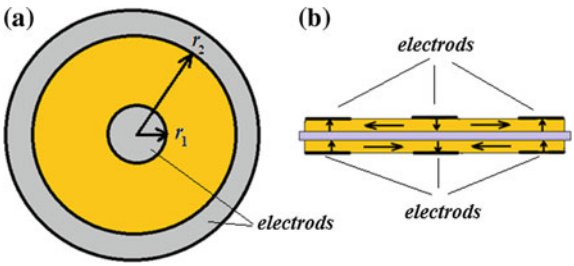

Fig. 26.1 **a** Piezoelectric element top view, axial section, **b** polarization scheme

(iii) Finite element modeling of PEG with an inhomogeneously polarized piezoelement;
(iv) Numerical and analytical calculation of the output characteristics of the power harvesting device;
(v) Optimization of the structural characteristics of PEG for obtaining its greatest efficiency.

26.2 Research Method

26.2.1 Continuous Formulation of the Problem

The mathematical model of flexural steady vibrations of a bimorph circular plate can be reduced to the boundary problem of electro-elasticity, which consists of a system of differential equations [11, 12].

We assume that the following constitutive equations are satisfied (piezoelectric medium is $\Omega_j = \Omega_{pk}$):

$$\rho_{pk}\ddot{\mathbf{u}} + \alpha_{dj}\rho_j\dot{\mathbf{u}} - \nabla\cdot\boldsymbol{\sigma} = \mathbf{f}_j; \quad \nabla\cdot\mathbf{D} = 0, \tag{26.1}$$

$$\boldsymbol{\sigma} = \mathbf{c}_j^E\cdot\cdot(\boldsymbol{\varepsilon} + \beta_{dj}\dot{\boldsymbol{\varepsilon}}) - \mathbf{e}_j^T\cdot\mathbf{E}; \quad \mathbf{D} + \varsigma_d\dot{\mathbf{D}} = \mathbf{e}_j\cdot\cdot(\boldsymbol{\varepsilon} + \varsigma_d\dot{\boldsymbol{\varepsilon}}) + \mathfrak{э}_j^S\cdot\mathbf{E}, \tag{26.2}$$

$$\boldsymbol{\varepsilon} = (\nabla\mathbf{u} + \nabla\mathbf{u}^T)/2; \quad \mathbf{E} = -\nabla\varphi, \tag{26.3}$$

where $\rho(x, t)$ is the continuous function of coordinates (density); $\mathbf{u}(x)$ is the displacement vector-function; $\boldsymbol{\sigma}$ is the stress tensor, $\mathbf{f}$ are the mass forces vector; $\mathbf{D}$ is the electric induction vector; $\mathbf{c}_j^E$ is the elastic constant tensor; $\mathbf{e}_j$ is the tensor of piezoelectric constants; $\boldsymbol{\varepsilon}$ is the strain tensor; $\mathbf{E}$ is the electric field vector; $\varphi(x)$ is the electric potential function; $\mathfrak{э}_j^S$ is the dielectric permittivity tensor; α_{dj}, β_{dj}, ζ_d are non-negative damping coefficients, and the other symbols are the standard designations for theory of electroelasticity with the exception of index "j", corresponding to area Ω_j. (For elastic media $\Omega_j = \Omega_e$, the piezomodules $\mathbf{e}_j$ are equal to zero.)

For the media $\Omega_j = \Omega_{em}$ with pure elastic properties, only stress fields would be considered. Similar (26.1)–(26.3) and constitutive relationships are used, neglecting electric fields and piezoelectric connectivity effects. Equations (26.1)–(26.3) are added to the mechanical and electrical boundary conditions, as well as the initial conditions in the case of non-stationary problem. Numerical modeling of devices that can be described with (26.1)–(26.3) are performed using finite element method.

The boundary conditions are divided into mechanical and electrical. In particular, for an electrode (S_e), included in external circuit, besides the condition of constancy of the electric potential, which presents itself unknown function in this case, it is necessary to add the condition, defining electric current passes through this electrode:

$$\int_{S_e} \dot{D}_m ds = I. \tag{26.4}$$

In addition to previous equations, all material properties are handled as functions of coordinates:

$$\rho_k = \rho_{pk}(x); \quad \mathbf{c}_j^E = \mathbf{c}_j^E(x); \quad \boldsymbol{\varepsilon}_{\mathbf{a}j}^S = \boldsymbol{\varepsilon}_{\mathbf{a}j}^S(x); \quad \mathbf{e}_j^T = \mathbf{e}_j^T(x), \tag{26.5}$$

where we have

$$g = g^i + |P|(g^a - g^i), \text{ for tensors } \mathbf{c}_j^E \text{ and } \mathfrak{d}_j^S; \text{ and } g = |P|g^a, \text{ for tensor } \mathbf{e}_j^T. \tag{26.6}$$

Here g are corresponding tensor components, i points isotropic state, a points anisotropic state. Tensor of piezoconstants $\mathbf{e}_j^T$ will be zero for isotropic bodies. In previous paper [4], we presented specific modules of ACELAN software for describing, presenting and modeling the non-homogeneous polarization.

The matrices of elastic constants, piezoelectric constant and permittivity have the corresponding forms for regions with transverse polarization, respectively:

$$\begin{bmatrix} c_{11} & c_{12} & c_{13} & 0 & 0 & 0 \\ c_{12} & c_{11} & c_{13} & 0 & 0 & 0 \\ c_{13} & c_{13} & c_{33} & 0 & 0 & 0 \\ 0 & 0 & 0 & c_{44} & 0 & 0 \\ 0 & 0 & 0 & 0 & c_{44} & 0 \\ 0 & 0 & 0 & 0 & 0 & \frac{1}{2}c_{11} - \frac{1}{2}c_{12} \end{bmatrix}; \quad \begin{bmatrix} 0 & 0 & e_{31} \\ 0 & 0 & e_{31} \\ 0 & 0 & e_{33} \\ 0 & e_{15} & 0 \\ e_{15} & 0 & 0 \\ 0 & 0 & 0 \end{bmatrix}; \quad \begin{bmatrix} g_{11} & 0 & 0 \\ 0 & g_{11} & 0 \\ 0 & 0 & g_{33} \end{bmatrix}. \tag{26.7}$$

For regions with polarization in radial direction, we have another forms:

$$\begin{bmatrix} c_{33} & c_{13} & c_{13} & 0 & 0 & 0 \\ c_{13} & c_{11} & c_{12} & 0 & 0 & 0 \\ c_{13} & c_{12} & c_{11} & 0 & 0 & 0 \\ 0 & 0 & 0 & \frac{1}{2}c_{11} - \frac{1}{2}c_{12} & 0 & 0 \\ 0 & 0 & 0 & 0 & c_{44} & 0 \\ 0 & 0 & 0 & 0 & 0 & c_{44} \end{bmatrix}; \quad \begin{bmatrix} e_{33} & 0 & 0 \\ e_{31} & 0 & 0 \\ e_{31} & 0 & 0 \\ 0 & 0 & 0 \\ 0 & 0 & e_{15} \\ 0 & e_{15} & 0 \end{bmatrix}; \quad \begin{bmatrix} g_{33} & 0 & 0 \\ 0 & g_{11} & 0 \\ 0 & 0 & g_{11} \end{bmatrix}. \tag{26.8}$$

26.2.2 Technology of Piezoelements Polarization

Polarization of the piezoelement is performed in two stages using technological electrodes on the lower surface, which are removed after the second stage. Calculation of the residual polarization field is conducted in the finite element software ACELAN [7]. Figure 26.2 shows half of the axial section of the upper piezoceramic disk and two polarization stages: the first stage involves transverse polarization of the regions, covered by the electrodes (Fig. 26.2a), and the second stage involves polarization in radial direction of the section between them (Fig. 26.2b).

The lower piezoceramic disk is polarized in a similar way to the circuit, shown in Fig. 26.2 ($-V_0$ is replaced on $+V_0$).

26.2.3 Applied Theory of Flexural Axisymmetric Vibrations of PEG

Under the assumption of Kirchhoff-Love hypotheses for mechanical quantities and a single normal, the angle of inclination of the normal ϑ, radial and circular deformation, expressed through the deflection $U_z = U_z(r)$ of the median surface, takes the form, respectively:

$$\vartheta = -\frac{dU_z(r)}{dr}, \quad \varepsilon_r = -\frac{d^2U_z(r)}{dr^2}z, \quad \varepsilon_t = -\frac{1}{r}\frac{dU_z(r)}{dr}z. \tag{26.9}$$

Electrical potential distribution in parts with transverse polarization is found as

$$\varphi(r,\theta,z) = V_p\frac{z}{2h}\left(1-\frac{2z}{h}\right) + V_m\frac{z}{2h}\left(1+\frac{2z}{h}\right) + \Phi(r)\left(1-\frac{4z^2}{h^2}\right). \tag{26.10}$$

where h is the plate thickness; V_m, V_p are the electrical potentials on the upper and lower electrodes, respectively.

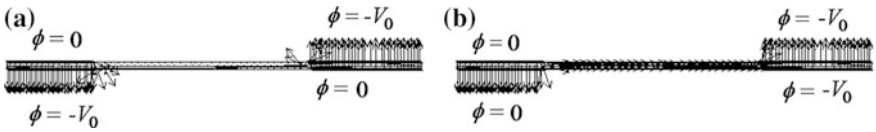

Fig. 26.2 First (**a**) and second (**b**) stages of piezoelement polarization

In a ring with polarization in radial direction, we have:

$$\varphi(r,\theta,z) = \Phi(r). \tag{26.11}$$

System of differential equations for areas with transverse polarization for a two-layer piezoactive bimorph for deflection $U_z = U_z(r)$ and the electric potential of the mid-surface $\Phi = \Phi(r)$ will take the forms:

$$\frac{d^4U_z}{dr^4}D + 2D\frac{1}{r}\frac{d^3U_z}{dr^3} - D\frac{1}{r^2}\frac{d^2U_z}{dr^2} + D\frac{1}{r^3}\frac{d^2U_z}{dr^2} - F\frac{d^2\Phi}{dr^2} - F\frac{1}{r}\frac{d\Phi}{dr} - \omega^2\rho h U_z = p(r); \tag{26.12}$$

$$\frac{d^2\Phi}{dr^2} - 3G\frac{d^2U_z}{dr^2} - G\frac{1}{r}\frac{dU_z}{dr} + H(-V_m + V_p - 4\Phi) = 0, \tag{26.13}$$

where $H = 3\frac{c_{33}g_{33}+e_{33}^2}{h^2 g_n c_{33}}$, $F = \frac{2h}{3}\frac{(c_{13}e_{33}-c_{33}e_{31})}{c_{33}}$, $G = \frac{c_{13}e_{33}-c_{33}e_{31}}{2g_{11}c_{33}}$, ω is the angular frequency of vibration.

Internal mechanical (M_r is the moment, Q_r is the transverse force) and electrical (φ is the electric potential, D_r is the electric induction) factors are expressed as

$$\begin{aligned} M_r &= -D\left(\frac{d^2U_z}{dr^2} + \frac{1}{r}\frac{dU_z}{dr}\right) - \frac{h^3}{18}(-V_m + V_p - 4\Phi)H; \\ Q_r &= -D\left(\frac{d^3U_z}{dr^3} + \frac{1}{r}\frac{d^2U_z}{dr^2} - \frac{1}{r}\frac{dU_z}{dr}\right) - J\frac{d\Phi}{dr}; \end{aligned} \tag{26.14}$$

$$\varphi = \frac{1}{12}(-V_m + V_p + 8\Phi); \quad D_r = -\frac{2}{3}g_{11}\frac{d\Phi}{dr}, \tag{26.15}$$

where $J = \frac{2}{3}h\frac{(c_{33}e_{15}-c_{13}e_{33}+c_{33}e_{31})}{c_{33}}$.

For a region with longitudinal polarization, the system of differential equations corresponding to the system (26.11), (26.12) has the form:

$$D_1\frac{d^4U_z}{dr^4} + 2D_1\frac{1}{r}\frac{d^3U_z}{dr^3} - D_2\frac{1}{r^2}\frac{d^2U_z}{dr^2} + D_2\frac{1}{r^3}\frac{dU_z}{dr} - F_1\frac{d^3\Phi}{dr^3} - F_2\frac{1}{r}\frac{d^2\Phi}{dr^2} - \omega^2\rho h U_z = p(r); \tag{26.16}$$

$$K\frac{d^2\Phi}{dr^2} + L\frac{d^3U_z}{dr^3} - N\frac{1}{r}\frac{d^2U_z}{dr^2} + N\frac{1}{r^2}\frac{dU_z}{dr} = 0; \tag{26.17}$$

where

$$D_1 = \frac{h^3}{12}\frac{(c_{11}c_{33} - c_{13}^2)}{c_{11}}; \quad D_2 = \frac{h^3}{12}\frac{(c_{11}^2 - c_{12}^2)}{c_{11}}; \quad F_1 = \frac{h^2}{4}\frac{(c_{11}e_{33} - c_{13}e_{31})}{c_{11}};$$
$$N = \frac{h}{4}\frac{(c_{12}e_{31} - c_{11}e_{31})}{c_{11}}; \quad F_2 = \frac{h^2}{4}\frac{(2c_{11}e_{33} - c_{13}e_{31} + c_{12}e_{31} - 2c_{13}e_{31})}{c_{11}};$$
$$K = \frac{(c_{11}g_{33} + g_{31}^2)}{c_{11}}; \quad L = \frac{h}{4}\frac{(c_{11}e_{33} - c_{13}e_{31})}{c_{11}}.$$

Internal mechanical and electrical factors are expressed as

$$M_r = -D_1\frac{d^2U_z}{dr^2} - D_3\frac{1}{r}\frac{dU_z}{dr} + F_1\frac{d}{dr}\Phi;$$
$$Q_r = -D_1\frac{d^3U_z}{dr^3} - D_1\frac{1}{r}\frac{d^2U_z}{dr^2} + D_2\frac{1}{r^2}\frac{dU_z}{dr} + F_1\frac{d^2\Phi}{dr^2} + F_3\frac{1}{r}\frac{d\Phi}{dr}; \tag{26.18}$$

$$\varphi = \Phi(r); \quad D_r = \frac{1}{h}F_1\frac{d^2U_z}{dr^2} + N\frac{1}{r}\frac{dU_z}{dr} - K\frac{d}{dr}\Phi, \tag{26.19}$$

where

$$D_3 = -\frac{h^3}{12}\frac{(c_{11}c_{13} - c_{12}c_{13})}{c_{11}}, F_3 = \frac{h^2}{4}\frac{(c_{11}e_{33} - c_{13}e_{31} - c_{11}e_{31} + c_{12}e_{31})}{c_{11}}.$$

The boundary conditions and congruence conditions have the forms:

for $r = 0$:
$\vartheta = 0$ and in the absence of concentrated force or inertial mass, we have
$Q_r = 0$ from (26.14) and $D_r = 0$ from (26.13);
for $r = r_i$, $i = 1, 2$, we have congruence of parts with different polarizations.

The conditions for continuity of deflections U_z, angles ϑ, moments and transverse forces, we obtain from (26.14) and (26.18), electric potential and electrical induction are found from (26.15) and (26.19).

26.3 Results and Discussion

26.3.1 Static Load

Next, the efficiency of a uniformly and inhomogeneously polarized PEG is compared. The thickness of the piezolayers (from PZT-4) is equal to 0.2 mm, the radius is 19 mm, the thickness of the steel plate, on which they are pasted, equals 0.1 mm. The load is a uniform pressure with intensity of 1 kPa. For piecewise constant polarization, the dimensions of the electrodes vary.

Table 26.1 Static load

No.	Type of PEG and sizes of electrodes (mm)	Deflection at the center (mm)	Output potential (V)
1	Uniform polarization	0.5×10^{-3}	0.85
2	Inhomogeneous polarization $r_1 = 3$, $r_2 = 6$	0.54×10^{-3}	13.82
3	Inhomogeneous polarization $r_1 = 2$, $r_2 = 7$	0.58×10^{-3}	21.4
4	Inhomogeneous polarization $r_1 = 1$, $r_2 = 8$	0.62×10^{-3}	28.3

Table 26.1 presents the results of calculation of deflection and output potential for PEG with homogeneous polarization (No. 1) and for different electrode sizes (Nos. 2–4).

26.3.2 Steady-State Vibrations

Steady-state vibrations of the PEG at the first antiresonance frequency are considered. The shape of the vibrations, with the distribution of the axial displacement, is shown in Fig. 26.3a, the distribution of the electrical potential for homogeneous polarization (No. 1 in Table 26.2) is shown in Fig. 26.3b, and for the inhomogeneous polarization (No. 3 in Table 26.2), it is shown in Fig. 26.3c.

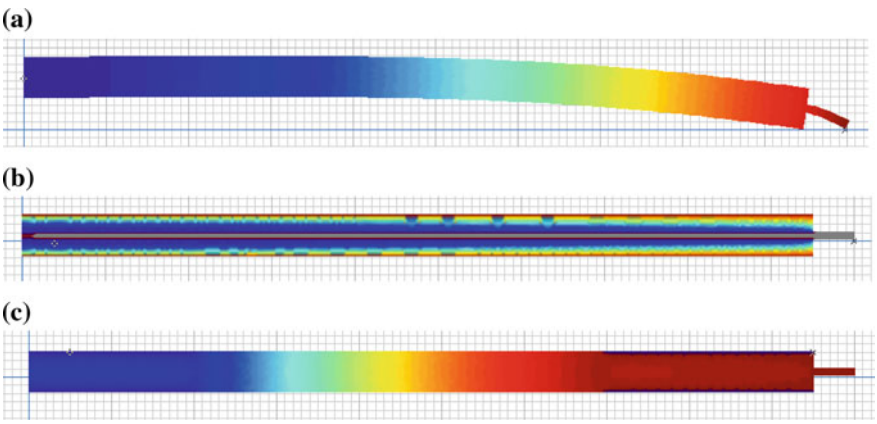

Fig. 26.3 Distributions of deflection (**a**) and electric potential (**b**) at homogeneous polarization, (**c**) inhomogeneous polarization

Table 26.2 Harmonic analysis

No.	Type of PEG and sizes of electrodes (mm)	Antiresonance frequency (kHz)	Deflection at the center (mm)	Output potential (V)
1	Uniform polarization	4.528	2.34×10^{-3}	37.8
2	Inhomogeneous polarization $r_1 = 3$, $r_2 = 6$	4.350	2.51×10^{-2}	617
3	Inhomogeneous polarization $r_1 = 2$, $r_2 = 7$	4.200	2.66×10^{-2}	939
4	Inhomogeneous polarization $r_1 = 1$, $r_2 = 8$	4.095	2.77×10^{-2}	1221

Table 26.2 shows the calculation results for the first antiresonance frequency: the deflection at the center and the output potential for PEG with homogeneous polarization No. 1 and for different electrode sizes Nos. 2–4.

26.4 Conclusion

An applied theory of axisymmetric vibrations of PEG with a piecewise constant polarization is constructed. The results of the calculations show the significant efficiency of PEG with regions of polarization in radial direction, when generating an output potential in comparison with PEG with homogeneous polarization of piezoceramic layers. It is shown that the output potential increases with the growth of the region with polarization in radial direction. There is a limiting size of this section, which can be efficiently polarized. So, it is possible to make several such sections of a given size to create an effective device.

Acknowledgements This research was performed into framework of financing RFBR grant number 16-01-00354A.

References

1. A.N. Solovyev, L.V. Duong, Int. J. Appl. Mech. **8**(3), 1650029 (2016)
2. L.V. Duong, M.T. Pham, V.A. Chebanenko, A.N. Solovyev, C.V. Nguyen, Int. J. Appl. Mech. **9**(6), 1750084 (2017)
3. A.N. Soloviev, I.A. Parinov, L.V. Duong, C.C. Yang, S.H. Chang, J.C.Y. Lee, in *Physics and Mechanics of New Materials and Their Applications*, ed. by I.A. Parinov, S.-H. Chang (Nova Science Publishers, New York, 2013), 147pp

4. V.A. Akopyan, I.A. Parinov, Y.N. Zakharov, V.A. Chebanenko, E.V. Rozhkov, in *Advanced Materials—Studies and Applications*, ed. by I.A. Parinov, S.H. Chang, S. Theerakulpisut (Nova Science Publishers, New York, 2015), 417pp
5. A.V. Belokon, A.S. Skaliukh, *Mathematical Modeling of Irreversible Processes of Polarization* (FizMatLit, Moscow, 2010), 328pp (in Russian)
6. A.S. Skaliukh, A.N. Soloviev, P.A. Oganesyan, Ferroelectrics **483**(1), 95 (2015)
7. A.N. Soloviev, P.A. Oganesyan, A.S. Skaliukh, in *Advanced Materials—Studies and Applications*, ed. by I.A. Parinov, S.H. Chang, S. Theerakulpisut (Nova Science Publishers, New York, 2015), 169pp
8. A.O. Vatulian, I.P. Getman, N.B. Lapnitskaya, Appl. Mech. **27**(10), 101 (1991)
9. A.O. Vatul'yan, A.A. Rynkova, J. Appl. Mech. Tech. Phys. **42**(1), 164 (2001)
10. A.N. Soloviev, P.A. Oganesyan, A.S. Skaliukh, Le V. Duong, V.K. Gupta, I.A. Panfilov, in *Advanced Materials—Techniques, Physics, Mechanics and Applications*, vol. 193, Springer Proceedings in Physics, ed. by A. Parinov, S.-H. Chang, M.A. Jani (Springer Cham, Heidelberg, New York, Dordrecht, London, 2017), 473pp
11. A.V. Belokon, V.A. Eremeyev, A.V. Nasedkin, A.N. Solov'yev, J. Appl. Math. Mech. **64**(3), 367 (2000)
12. A.V. Belokon, A.V. Nasedkin, A.N. Solov'yev, J. Appl. Math. Mech. **66**(3), 481 (2002)